# Microstructural aspects of the fatigue behavior of rapid heat treated steel

Prof. T. KUNIO*, Assist. Prof M. SHIMIZU† and K. YAMADA*
* Dept. of Technology, Keio University, 4-5-11 Maebara-cho, Koganei-shi, Tokyo, Japan.
† Kyoto University of Industrial Arts and Textile Fibers, Matsugasaki, Sakyo-ku, Kyoto-shi, Japan.

## Summary
A study has been made of the initiation and propagation of microscopic fatigue cracks in mixed microstructures (ferrite and quenched microstructures such as martensite) quenched after rapid heating.

It is shown that fatigue cracks are formed and developed along slip bands in the retained ferrite, although these do not immediately lead to the fracture of the specimen because they are impeded by the surrounding microstructures. It was concluded that the fatigue limit of the rapidly heat-treated steel containing mixed microstructures, was the critical stress, at which cracks, formed in the retained ferrite, propagated through the surrounding microstructures and not the stress which initiated the crack. In addition, it was found that induced residual compressive stresses had no appreciable influence on the stress level at which cracks initiated in the retained ferrite, but did have a significant influence on the stress level at which they propagated through the surrounding microstructures.

## Introduction
In recent years, treatment such as ausforming [1, 2], and maraging [3], have been developed to obtain higher tensile and fatigue strengths without loss of ductility [4]. In these treatments, the emphasis is on the cooling operation, aging after quenching, and the addition of alloying elements to increase the effectiveness of this operation.

The heat treatment technique discussed here is known as induction-hardening and produces characteristic microstructures and mechanical properties [5]. Microstructures are composed of martensite, in which the carbon concentration is not constant in any area of the microstructure; this is a result of incomplete diffusion of carbon in the austenite region and gives rise to ferrite domains within the microstructure. Also, the appearance of martensite is not needlelike, but nodular. Induction-hardening increases both the static and fatigue strengths of a steel. Studies in fatigue strength improvement by induction-hardening has been made by Nakamura *et al.* [6], who concluded that their improvements are due to the macroscopic residual compressive stress in the surface layer of the specimen, and the increased strength of the microstructure.

The purpose of this paper is to investigate the metallurgical factors governing the fatigue strength of an induction hardened steel.

**Fatigue strength of mixed microstructures**

Some typical examples of the features of the microstructure of a rapidly heat-treated low carbon steel are shown in Fig. 1; the composition of the steel is shown in Table 1. The time required for specimens to reach 1000 °C varied between 3 and 25 sec., and in every condition, retained ferrite was observed in the microstructures. The domain of retained ferrite in the microstructures became narrower as the heating duration was lengthened. Hardness measurements, taken at random locations on the specimens are shown in Fig. 2. Rotating bending and reversed torsion fatigue tests were made on thin-walled specimens (Fig. 3). Thin walled specimens were used to avoid the generation of residual stresses by the rapid heating and cooling of the specimen, and to eliminate the effect of stress gradient. Residual stresses were measured by Sachs method, typical results are shown in Fig. 4. Their magnitude was considered sufficiently small to conclude that the fatigue behavior of the specimens would not be affected by their presence. The results of the fatigue tests are given in Figs. 5 and 6. They show that the fatigue limit of the specimens is independent of the heating duration, i.e., $\sigma_{w0} = 30$ kg/mm² (rotating fatigue limit) and $\tau_{w0} = 18$ kg/mm² (reversed torsion fatigue limit). The fatigue limits of annealed specimens are $\sigma_{w0} = 19$ kg/mm² and $\tau_{w0} = 12$ kg/mm², respectively.

It is well known that the rotating bending fatigue limit of rapidly heat treated low carbon steel solid specimens is approximately $\sigma_{w0} = 50$ to 60 kg/mm² [6]. Consequently, the fatigue limit of the thin walled hollow specimen used in this experiment is low, its value being approximately one half that of the solid specimens. It is considered that this is due to the elimination of residual compressive stresses in the thin walled specimens.

Microstructural changes due to fatigue stressing, are shown in Fig. 7. A stress level of $\sigma = 36$ kg/mm², which was 120% of the fatigue limit was applied. A fine slip marking first appeared within the domain of retained ferrite after about 1% of the fatigue life. This slip band gradually increased its width and depth with further fatigue stressing and progressively developed into a more intensified slip band [9] spanning the entire domain of retained ferrite (Fig. 7 (c), Fig. 7 (d)). After approximately 50% of the fatigue life, the slip bands had increased their width and depth to the stage where they could not be eliminated by light electropolishing [10] (Fig. 7 (e)). At this stage it was considered that they had already become micro fatigue cracks, and this was verified by applying the $\sigma = 100$ kg/mm² tensile stress (Fig. 7 (f)). Accordingly, it is evident that fatigue fracture commences in the retained ferrite of the mixed microstructures (Fig. 8), as appreciable changes were only observed in the domains of retained ferrite. With further fatigue stressing, the fatigue cracks in the retained ferrite propagated across the surrounding microstructures to final fracture.

The question arises as to whether the local fractures of the retained ferrite are a necessary and sufficient condition for the fracture of the bulk





specimen. The test results shown in Figs. 5 and 6 seem to confirm that it is. However, to investigate this point further the microstructural changes below the fatigue limit, in the retained ferrite domains were observed. The results of this investigation revealed that the microstructural changes observed below the fatigue limit in the retained ferrite were identical to those observed above the fatigue limit. Similar fractures occurred in the local domains of retained ferrite, but fracture of the bulk specimen did not occur (Fig. 9). Thus the suggestion that the fatigue limit of a specimen is the minimum stress required to fracture the retained ferrite is invalidated. To understand the significance of the fatigue limit of mixed microstructures, attention was focused on the microstructural changes which occur near the fatigue limit. It was observed that many microcracks were present in the retained ferrite at stresses from well below the fatigue limit up to the fatigue limit, and that all of the cracks were contained within the domain of retained ferrite, their propagation beyond these being impeded by surrounding microstructures. Consequently, the fatigue limit of mixed microstructures, containing retained ferrite, is the minimum stress required to propagate the fatigue cracks in the retained ferrite through the surrounding microstructures. Cracks in the retained ferrite could be regarded as 'stage I cracks', as proposed by Forsyth [11]; the cracks propagating into the surrounding microstructures could be regarded as 'stage II cracks', thus, the fatigue limit could be described as the critical stress required to cause a stage I crack in the retained ferrite to extend across the surrounding microstructures into a stage II crack.

**The latest possibility of crack origination in mixed microstructures**

Although retained ferrite in a rapidly heat treated microstructure governs fatigue strength, two points are of interest. (1) If a ferrite domain is extremely small, is it still the origin of fracture? and (2), even though a ferrite domain is extremely small and is the origin of fracture, are there any other possible sites for a fracture to start?

Details of the specimen used in this experiment are shown in Fig. 10, and Table 2. The maximum temperature of the rapid heat treatment specimens was controlled at 1100°C and the times required for the temperature to reach 1000 °C were selected as 10 and 15 sec. The 10 sec specimens (denoted by 10, IH) contained small quantities of retained ferrite, while the 15 sec specimen (denoted by 15 III) contained no retained ferrite, (Figs. 11 & 12). The results of rotating bending fatigue tests on these specimens are shown in Figs. 13 and 14. Microscopic observations of the 10 IH specimens revealed fine slip marking in the retained ferrite early in the life, which eventually developed into microcracks. At the fatigue limit, microcracks existed only within the retained ferrite. At stress levels $\sigma = 60$ kg/mm², cracks start in the retained ferrite final fracture being due

to the propagation of cracks in the retained ferrite extending across the surrounding microstructures (Figs. 15, 16). At stress levels above $\sigma$ = kg/mm², cracks which produced the final fracture originated in the microstructures surrounding the retained ferrite (Fig. 17). It was also observed that cracks which originated in the surrounding microstructure began to propagate to cause final fracture cracks began to grow in the retained ferrite. The above condition implies that the fatigue limit of the surrounding microstructures is approximately $\sigma$ = 60 kg/mm². However it can be considered that the 15 IH specimens consist entirely of the surrounding microstructures of the 10 IH specimens, excluding the retained ferrite. Consequently, the S-N curve for the 15 IH specimen could be interpreted as the crack nucleation curve of the surrounding microstructures of the 10 IH specimens. In the 15 IH specimens, the crack propagation period is short, so that it could be considered that the curve in Fig. 14 indicates the crack initiation curve of the surrounding microstructures of the 10 IH specimens. It now becomes apparent that the microstructures surrounding the retained ferrite has a fatigue limit, of $\sigma_{w0}$ = 40 kg/mm². If the fatigue limit of the surrounding microstructures in the 10 IH specimens is $\sigma_{w0}$ = 40 kg/mm², cracks would have been observed in the surrounding microstructures at stress levels in excess of $\sigma$ = 40 kg/mm². However, Fig. 18 which shows the S-N curve of the 15 IH specimens and can be considered the crack nucleation S-N curve of the surrounding microstructure of the 10 IH specimen, within the stress range of $\sigma$ = 40 to 60 kg/mm² (designated II in the figure), indicates that fracture in the surrounding microstructures may start at a later life than the onset of the growth of cracks from the retained ferrite into surrounding microstructure. Thus, in this stress range, there is a possibility of the initiation of cracks in the surrounding microstructure, although these have not been observed.

From these considerations, it could be concluded that the fatigue strength of rapid heat treated microstructures containing retained ferrite, is governed by three factors;

1. The initiation and propagation of cracks within the retained ferrite.
2. The possibility of crack initiation in the surrounding microstructure below a stress level of $\sigma$ = 60 kg/mm².
3. The initiation of cracks in the surrounding microstructure, above a stress level of $\sigma$ = 60 kg/mm².

**The effect of residual compressive stress on fatigue strength**

To clarify the effect of residual compressive stress, the fatigue behavior of solid specimens which were rapidly heat treated were compared with the results of the stress free hollow specimens. The chemical composition and shape of specimens used are shown in Fig. 9, and Table 3. In heat treating a specimen the time required for it to reach 1000°C. was valued





between 5 and 30 sec. and in every condition, retained ferrite was observed in the microstructure. Measurement by the Sachs method gave a value of $\sigma_r$ = −50 kg/mm² for the residual compressive stress in the surface layer of the specimen. The rotating bending fatigue limit of these specimens was about $\sigma_{w0}$ = 50 to 55 kg/mm². This value is 20 kg/mm² higher than the fatigue limit of the hollow specimens mentioned earlier. Microscopic observations revealed fine slip markings in the retained ferrite which gradually developed into micro fatigue cracks and propagated across the surrounding microstructures. However, a larger number of micro cracks, were found in the retained ferrite, in solid specimens tested at their fatigue limit ($\sigma_{w0}$ = 50 to 55 kg/mm²) than were found in hollow specimens tested at their fatigue limit. All cracks were actually observed in the retained ferrite, and no cracks which were in the process of breaking through the surrounding microstructures were detected. Thus, in the case of solid specimens $\sigma_{w0}$ = 50 to 55 kg/mm² corresponds to the critical stress to cause a stage 7 crack in the retained ferrite, to grow.

Stage I cracks or slip band cracks were observed in the retained ferrite below the fatigue limit of the hollow specimens. Microstructural observations of the solid specimens revealed stage I cracks at strikingly low stress levels of 30 to 35 kg/mm² ($N$ = $10^7$). In addition, the critical stress for the initiation of slip bands was at the low stress level of 22 to 24 kg/mm² ($N$ = $10^7$). This value is in agreement with that for the low carbon specimen mentioned earlier, although the fatigue limit of the solid specimens, which was considered to be the critical stress to start the cracks into stage II growth. is higher than that of hollow specimens. From this result and the fact that the difference of fatigue behavior between solid and hollow specimens could be due to the existence of residual compressive stresses, it can be concluded that the fatigue strength is raised by residual compressive stresses, which suppresses the propagation of stage I cracks in the retained ferrite into stage II cracks. To clarify the effects of residual compressive stresses few experiments were carried out.

Solid specimens were bored out to release the residual compressive stress. The results of fatigue tests on these hollow specimens are shown in Figs. 20-22 and are summarised in Fig. 23. It is seen that there is little difference between the critical stresses for stage I crack initiation slip band nucleation for both solid and hollow specimens. Consequently, it can be concluded that the residual compressive stresses have no appreciable influence on the origination of either slip bands or micro cracks. However consideration of the number of cycles to fracture shows that the fatigue strength is improved by the suppression of the development of stage II cracks. This was confirmed by the application of an external compressive stress of $\sigma$ = −30 kg/mm² to a hollow specimen tested at the stress level $\sigma$ = 50 kg/mm² by tightening up a through bolt. The specimen did not

fracture after $10^7$ cycles at this stress level which is 120% of the fatigue limit, implying that the critical stress of crack propagation was raised. Thus, it can be concluded that the fatigue strength of rapidly heat treated steel is improved by the existence of residual compressive stress, which suppresses the development of stage II cracks.

**Acknowledgements**

The authors are extremely grateful to Dr H. Nakamura and Dr H. Takahashi for their fruitful discussions and helpful suggestions. The authors are also indebted to the Japan Steel Works Ltd. for the preparation of material, and to the Staffs of the Material Science Laboratory, Keio University for their assistance in conducting the experiment.

**References**

1. ZACKAY, V. F., JUSTUSSEN, M. W. & SCHMATZ, D. J., 'Strengthening by martensitic transformation', *Strengthening Mechanisms of Solids*, A.S.M., Cleveland, p. 179, 1962.
2. SCHMATZ, D. J., SCHALLER, F. W. & ZACKAY, V. F., 'Structural aspects of martensite of high strength', *Proc. Conf. on the Relation between the Structure and Mechanical Properties of Metals*, H.M.S.O., 614, 1963.
3. DECKER, R. F., 'Maraging steel, structure-property relationships', *Proc. Conf. on the Relation Between the Structure and Mechanical Properties of Metals*, H.M.S.O., 648, 1963.
4. BORIK, F., JUSTUSSEN, W. M. & ZACKAY, V. F., 'Fatigue properties of an ausformed steel', *Trans. A.S.M.*, vol. 56, 327, 1963.
5. NISHIMURA, H., *Bull. Japan Inst. of Metals*, vol. 1, No. 8, 520, 1962.
6. NAKAMURA, H., 'Induction-hardening and fatigue strength', *Nikkan Kogyo Shinbun*, Yokyo, 1963.
7. KUNIO, T., NAKAMURA, H., & SHIMIZU, M., 'Crack propagation of notched specimen with residual compressive stress', *Proc. 1st Int. Conf. on Fracture*, 1597, 1965.
8. SHIMIZU, M., NAKAMURA, H. & KUNIO, T., *Trans. Japan Soc. Mech. Engr.*, vol. 34, No. 258, p. 230, 1968.
9. HEMPLE, M., 'Metallographic observations on the fatigue of steels', *Proc. Int. Conf. on Fatigue of Metals*', A.S.M.E., p. 543, 1956.
10. THOMPSON, N., 'Experiments relating to the origin of fatigue cracks', *Fatigue in Aircraft Structures*, Academic Press, p. 43, 1956.
11. FORSYTH, P. J. E., 'Fatigue damage and crack growth in aluminium alloys', *Acta Metallurgica*, vol. 11, p. 703, 1963-7.





(a) 1000°C, 5 sec.

(b) 1000°C, 12 sec.

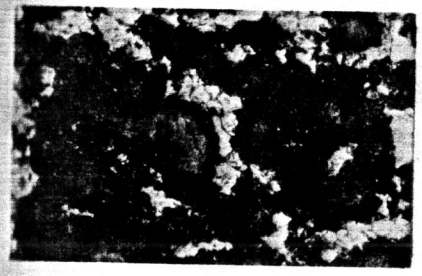

(c) 1000°C, 20 sec.

Fig. 1. Rapid heat treated microstructure (× 100)

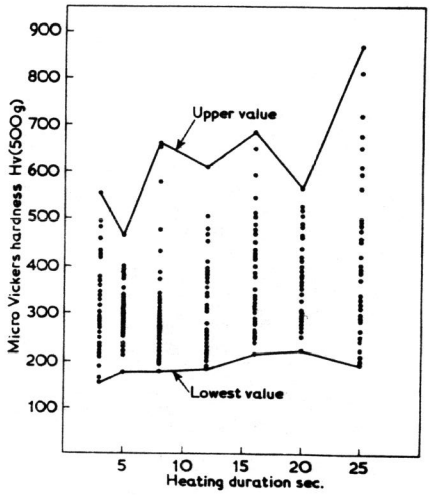


Fig. 2. Relations between the heating duration and distribution of hardness.

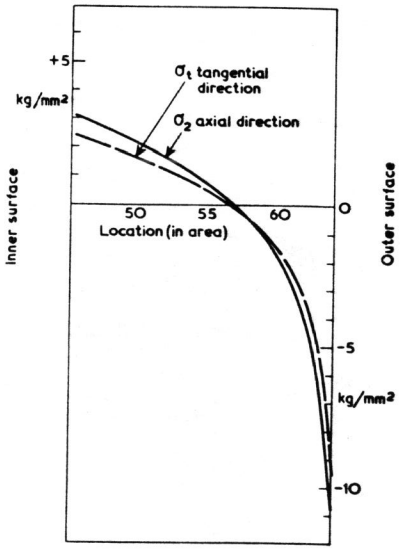


Fig. 4. Residual stress distribution heating duration 8 sec.

*Table 1. Composition of materials*

| | C | Si | Mn | S | P |
|---|---|---|---|---|---|
| S15C | 0·17% | 0·20% | 0·56% | 0·016% | 0·021% |

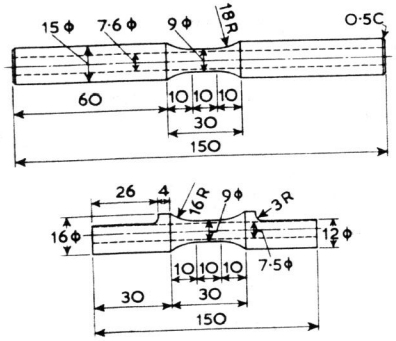


Fig. 3. Specimens

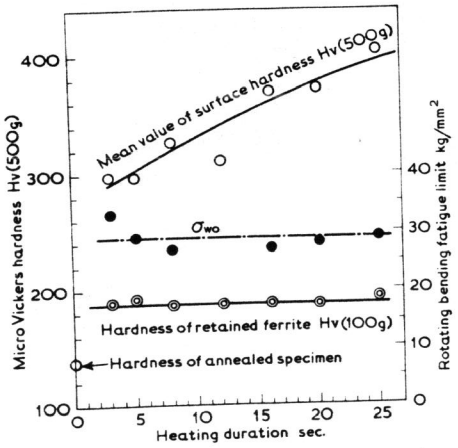


Fig. 6. Relations between the mean value of surface hardness retained ferrite and rotating bending fatigue limit

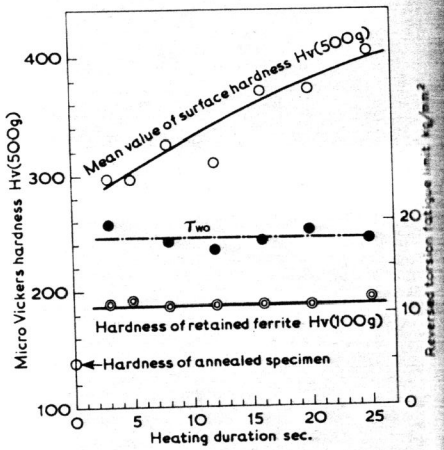


Fig. 5. Relations between the mean value of surface hardness, retained ferrite and reversed torsion fatigue limit.



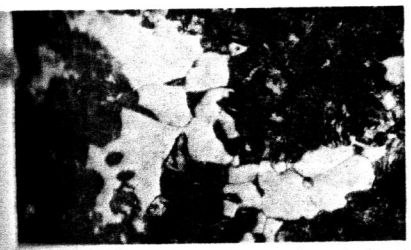

(a) $N = 0$, before fatigue stressing

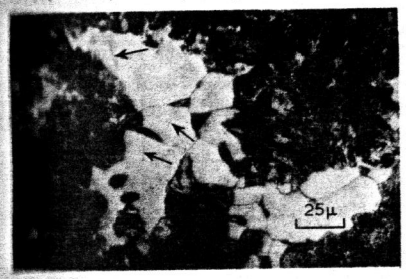


(b) $N = 2 \times 10^3$ slip marking first appeared (indicated by arrows)

(c) $N = 2 \times 10^4$

(d) $N = 10^5$ intensified slip bands

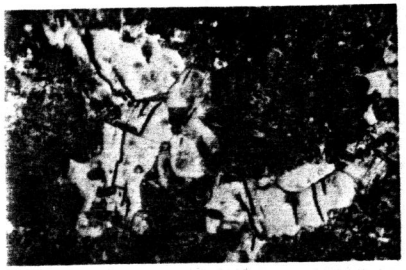

(e) $N = 10^5$ after light electropolishing

(f) $N = 10^5$ Micro fatigue cracks in the retained ferrite were revealed by the application of $\sigma = 100$ kg/mm² of tensile stress after electropolishing.

Fig. 7. Microstructural changes in the retained ferrite due to fatigue stressing on the 1000°C, 8 sec. specimen at the stress level of $\sigma = 36$ kg/mm² (120% of the fatigue limit) × 540.


Fig. 8. Characteristic feature of crack origination site (retained ferrite) after light electropolishing and the application of $\sigma = 100$ kg/mm² tensile stress $N = 2 \times 10^5$ (50% of fatigue life has been expended) $\sigma = 34$ kg/mm² 1000°C, 8 sec. specimen.


Fig. 9. $\sigma = 28$ kg/mm², $N = 10^7$ the crack, impeded its propagation by surrounding microstructures (non-propagating crack) after light electro-

Tab. 2. Chemical Composition

| C | Si | Mn | P | S |
|---|---|---|---|---|
| 0·36% | 0·27% | 0·53% | 0·011% | 0·014% |

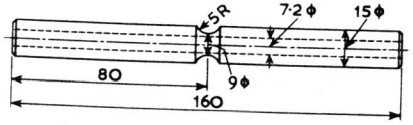


Fig. 10. Specimen.

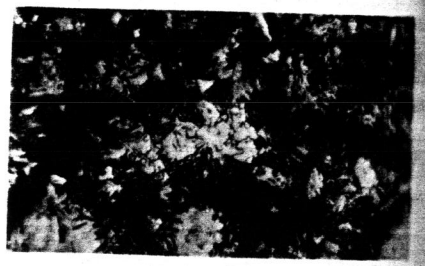

Fig. 11. Micrograph of 10 IH specimen (× 270). Retained ferrite domain is appeared white at the center position, while the other white domain, center low is the martensite which is difficult to etch by dilute nitric acid solution.

Fig. 12. Micrograph of 15 IH specimen (× 270). White domain, the center and right, is the martensite which is difficult to etch by dilute nitric acid solution.

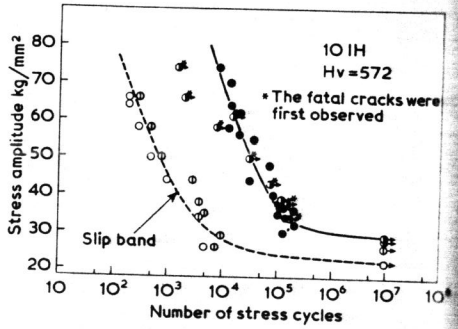


Fig. 13. Result of rotating bending fatigue test (10 IH Specimens).

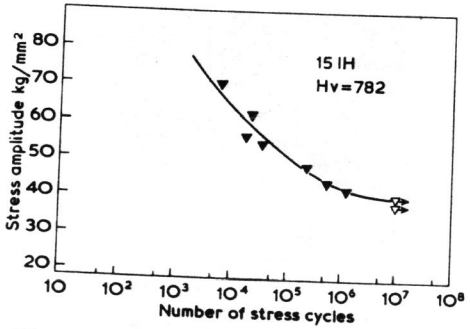


Fig. 14. Result of rotating bending fatigue test (15 IH Specimens).






← Surrounding microstructure (martensite) Hv > 750

← Retained ferrite Hv = 200

Fig. 15. Crack in the retained ferrite, began to propagatate to cause a final fracture $\sigma = 50$ kg/mm², $N = 3 \times 10^4$.

Fig. 16. The commencement of propagation of slip band crack in the retained ferrite into the surrounding microstructure.
× 270
$\sigma = 50$ kg/mm²
$N = 3 \times 10^4$


Fig. 17. Crack originated in the surrounding microstructure (martensite).
$\sigma = 74$ kg/mm²
$N = 1{\cdot}5 \times 10^3$
× 270

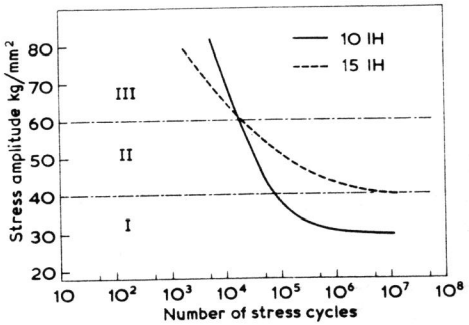


Fig. 18. The latent possibility of crack origination in martensite.

*Table 3. Chemical composition*

| C | Si | Mn | P | S |
|---|---|---|---|---|
| 0·13% | 0·24% | 0·74% | 0·016% | 0·032% |

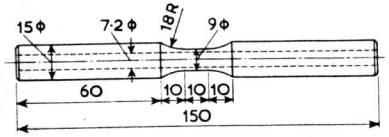


Fig. 19. Specimens.

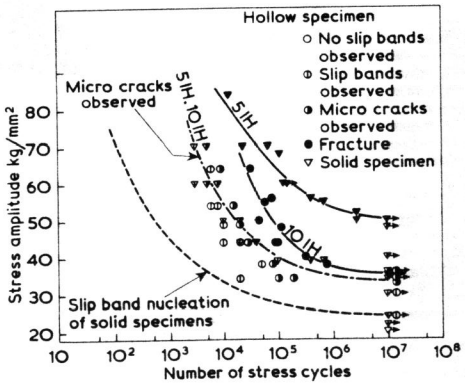


Fig. 20. Rotating bending fatigue test of solid and hollow specimens.





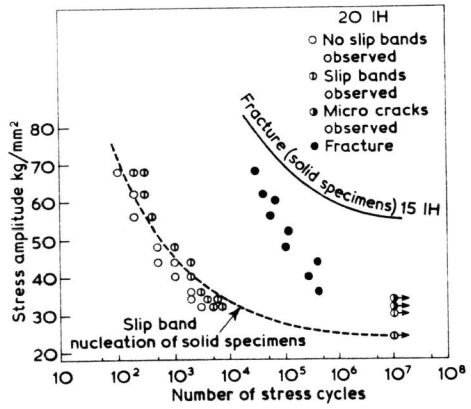


Fig. 21. Rotating bending fatigue test of hollow specimens.

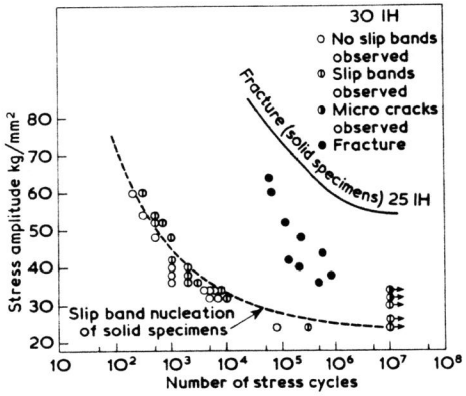


Fig. 22. Rotating bending fatigue test of hollow specimens.

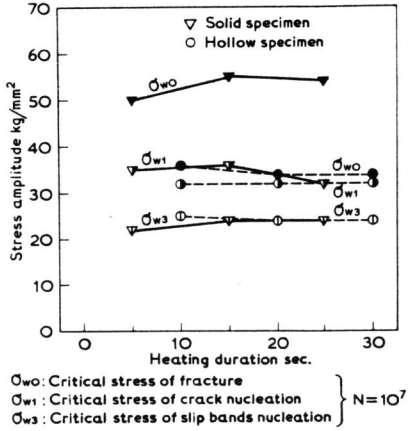


Fig. 23. Result of fatigue tests of both solid and hollow specimens.